Optik 127 (2016) 3918–3924

Contents lists available at ScienceDirect

Optik

journal homepage: www.elsevier.de/ijleo

Trap characteristics of UV-activated $Y_3(Al,Ga)_5O_{12}:Ce^{3+}$ phosphors

A.H. Wako[a,*], F.B. Dejene[a], H.C. Swart[b]

[a] Department of Physics, University of the Free State, QwaQwa Campus, Private Bag X13, Phuthaditjhaba 9866, South Africa
[b] Department of Physics, University of the Free State, P O Box 339, Bloemfontein ZA-9300, South Africa

ARTICLE INFO

Article history:
Received 23 September 2015
Accepted 28 December 2015

Keywords:
Peak maximum
Heating rate
Trap depth
Fast decay
Temperature

ABSTRACT

This paper reports on the trap characteristics of commercially obtained $Y_3(Al,Ga)_5O_{12}:Ce^{3+}$ phosphor powder. The effects of UV irradiation time and different heating rates have been discussed using different thermoluminescence (TL) techniques. In the TL glow curves of the $Y_3(Al,Ga)_5O_{12}:Ce^{3+}$ phosphor measured in the temperature range between room temperature (RT) and 250 °C, two TL peaks were observed, a maximum centered around 74 °C and a shoulder at around 163 °C when excited with UV radiation. Varying the UV irradiation (exposure) time or hence absorbed dose and heating rate significantly affected the peak intensity (I_m) and peak temperature (T_m) of the glow curve. The UV exposure time was varied from 3 min to 20 min and we noted that the TL intensity increased with UV exposure time in the range 3–15 min. This may be explained on the basis of second order recombination kinetics taking place due to a re-trapping process of the excitation. The intensity of the two TL peaks moved to the higher temperature side with an increase in the heating rate. The kinetic parameters at various heating rates namely activation energy (E), order of kinetics (b) and frequency factor (s) of the $Y_3(Al,Ga)_5O_{12}:Ce^{3+}$ sample were determined by the variable heating rate method, peak shape method and TL Anal Glow Curve Deconvolution (GCD) techniques.

1. Introduction

In recent years, oxide materials based on the garnet structure have attracted a lot of scientific and industrial interest around the world, as they offer excellent properties such as wide band gap, good chemical, thermal and radiation resistance and excellent radiation conversion efficiency [1]. Being one of the most common host materials, yttrium aluminum garnet ($Y_3Al_5O_{12}$, or YAG) has been studied for a variety of applications, for example general lighting, cathode ray tubes (CRT's), solid-state lasers and scintillators [2] among many others.

Thermoluminescence (TL) is the emission of light from insulators or semiconductors when they are thermally stimulated following the previous absorption of energy from radiation [3]. TL measurement is a very important and convenient method of investigating materials and provides important information on the nature of the traps, trapping energies and de-trapping mechanisms in crystals [4]. During TL measurements the TL spectrum is obtained by initially filling the traps at low (room) temperatures using UV or other radiation and then raising the temperature at a constant heating rate (β) [5]. The monochromatic radiation does the work of exciting electrons from within the band gap into the conduction band (CB) generating free charge carriers (electrons and holes) which may be captured in available trapping centers and occupy levels at a trap depth (E_t) below the CB [6]. The radiation dislodge electrons within the lattice structure of the material and the trapped electrons return to their normal, stable lower-energy positions, releasing energy during the TL heating process [7].

When activated with the right amount and type of radiation, it was confirmed that the rare-earth (RE^{3+}) ions such as co-dopants work as traps of photo-carriers within the band gap of the material [8]. Formation of an electron or a hole- trap by a defect depends on the energy level position of the RE^{3+} ions within the host band gap [9]. The charge carriers trapped at different depths causes various decay components, because the recombination between the excited electron and trapped hole is influenced greatly by the trap depth (E_t) [10]. If the depth of trap level is too shallow, the phosphor would exhibit fast decay or fluorescence and if it is too deep, the phosphor would hardly show any luminescence at room temperature. Hence, it is important for a material to have trapping level at a suitable depth in relation to the thermal release rate at room temperature [5]. The life time of the phosphor is dictated by the activation energy or trap depth of the hole/electron captured by the RE^{3+} ions and the intensity of the phosphorescence is

* Corresponding author. Tel.: +27 54727864167; fax: +27 587185444.
E-mail address: alihwako@gmail.com (A.H. Wako).

http://dx.doi.org/10.1016/j.ijleo.2015.12.155
0030-4026/

determined by the density or amount of the trapped holes/electrons and the rate of decay.

TL spectrum shows glow intensity as a function of temperature resulting in what is known as a glow curve. Analysis of the glow curve is one of the most significant ways to measure the number of traps and also the activation energy of the trap levels in luminescent materials. The TL glow curve is associated with the trap levels situated at different depths in the band gap between the conduction (CB) and the valence bands (VB) of a solid [11]. The depth of the traps (E_t) and their concentration (n_o) in the phosphors can be obtained by analyzing the TL spectrum [12]. The depth of each trap can be estimated from the peak temperature. Usually glow curves above room temperature feature one or several distinguished peaks and the energy corresponding to the glow peak is equal to the trap depth.

Several reports are available on the different TL techniques used to monitor the trapping states in materials such as initial rise method [2,4,7], glow curve deconvolution (GCD) [13] and peak shape method [12,14]. In this paper we use the variable heating rate method, peak shape method and TL Anal Glow Curve Deconvolution (GCD) program to determine the activation energies, trap depths, pre-exponential or frequency factor (s) of the traps associated with corresponding TL peaks in a commercially obtained $Y_3(Al,Ga)_5O_{12}:Ce^{3+}$ phosphor.

2. Experimental

Samples of commercially available $Y_3(Al,Ga)_5O_{12}:Ce^{3+}$ phosphor powders were obtained from Phosphor Technology (UK). The structure and phase composition were determined using a Bruker-AXS D8 Advance X-ray diffractometer (Bruker Corporation of Germany) operating at 40 kV and 40 mA using Cu Kα = 0.15406 nm from 15° to 65° (2θ), with a scan rate of 0.39° (2θ)/min and step scans with a step size of 0.02° (2θ). The room temperature photoluminescence (PL) excitation and emission fluorescence spectra were recorded using an F-7000 FL Spectrophotometer at scan speed of 60 nm/min at 400 PMT voltage and excitation and emission monochromator slit widths of 5 nm. The TL studies were carried out above room temperature using a TL 10091 Thermoluminescence Reader system with PMT type 9924 B supplied by M/s Nucleonix Systems Pvt. Ltd., India interfaced to a PC where the TL signals were analyzed to investigate traps and defects in the phosphor powders. The PMT tube has sufficient response over a wide spectral range. In order to fill the available traps, the samples were at first excited for 3, 5, 10 and 15 min using a 254 nm UV radiation standard lamp with a power of 15 W. Then the radiation source was removed and the samples were heated at various linear rates of 0.5, 0.8, 1.0, 1.2, 1.6, 2 and 2.5 °C/s to induce thermal release or de-trapping of the charge carriers. By varying the temperature as a function of the intensity, the TL spectrum was obtained displaying the integrated TL yield. During all the TL experiments, 20 mg of the sample was used and the glow peaks were recorded from RT to 300 °C.

3. Results and discussions

3.1. XRD analysis

XRD pattern and standard of the $Y_3(Al,Ga)_5O_{12}:Ce^{3+}$ phosphor powder is shown in Fig. 1. The peaks indexed well with the JCPDS card number 89-6660. It has a bcc structure of space group I a-3d (230) with 160 atoms in the cubic (primitive) cell and cell parameters; $a = 12.1552(6)$ Å; $\beta = 90°$, cell ratio; $a/b = 1.0$, $b/c = 1.0$, $c/a = 1.0$ and cell volume 1795.92 Å^3.

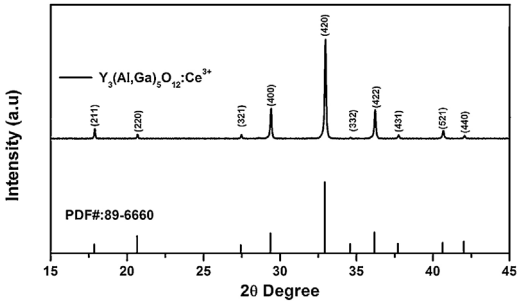

Fig. 1. XRD pattern of the $Y_3(Al,Ga)_5O_{12}:Ce^{3+}$ phosphor powder indexed with JCPDS card # 89-6660.

3.2. PL analysis

Fig. 2(a) and (b) show the PL excitation and emission spectra recorded from the as-prepared commercially obtained $Y_3(Al,Ga)_5O_{12}:Ce^{3+}$ powders. The PL emission spectra from the powder sample with a maximum in the yellow region at 560 nm is a broad band ranging from 550 nm to 650 nm corresponding to the 440 nm blue excitation due to the 4f-5d electronic transition of Ce^{3+} attributed to the de-localization of electrons from the lowest 5d level to the crystal field split 4f ($^2F_{5/2}$/$^2F_{7/2}$) levels of Ce^{3+}.

3.3. TL glow curves

Room temperature TL glow curves of the $Y_3(Al,Ga)_5O_{12}:Ce^{3+}$ recorded after irradiation with different UV exposure times as the temperature was increased linearly as a function of time at the rate of 1 °C/s are shown in Fig. 3. The intensity of the glow curves is already high at room temperature due to contributions from the photoluminescence effect of the UV excited $Y_3(Al,Ga)_5O_{12}:Ce^{3+}$ phosphor material whereby as soon as the UV irradiation stops the filled electron traps begin to empty starting with room and as the temperature is increased during the TL process. The glow curves consists of two thermal peaks each indicating that more than one type of trap is involved.

From the fitted glow curve of Fig. 3(b), the main peak is centered at 74 °C and the other on the higher temperature side at 163 °C suggesting availability of two un-equivalent trap types; shallow and deep respectively. The peak at around 74 °C is intense which is an indication of the presence of a sufficient number of shallow traps (trap 1) which means that the charge carriers do not migrate far away from the conduction band (CB) thus bringing about fast decay and the shoulder at around 163 °C suggests the existence of a fewer deep traps (trap 2) which could be responsible for longer decay times or no emission owing to its depth. It has also been shown that Ce^{3+} favors fast decay times as short as 25–30 ns [15] and can therefore be ascribed to the shallow traps at 74 °C since the trap depth is directly proportional to the maximum glow peak.

As can be seen from Fig. 3, the form of the glow curves remains the same without any observable change, except for a slight shift in peak positions, as we increased the UV dose. It has been reported that the large unit cell of YAG is prone to many defect sites and impurities especially at high temperatures due to a resultant lattice strain which arise from the presence of other RE^{3+} ion impurities or heterovalent impurity species [16].

Luminescence involves two kinds of active centers: emitters and traps. In $Y_3(Al,Ga)_5O_{12}:Ce^{3+}$ crystals Ce^{3+} is an emitter, while Al^{3+} and Ga^{3+} form substitutional defects that serve as trapping centers. The faster decay speed or fluorescence emission of Ce^{3+} is due to the existence of shallow traps nearby Ce^{3+} ions. When Ce^{3+} is excited with UV radiation generating free charge carriers (electrons and holes), electrons in the valence band (VB) of the host lattice or the

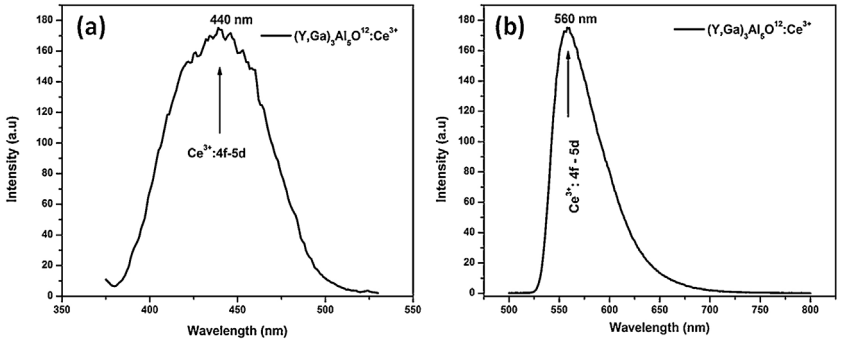

Fig. 2. Room temperature PL excitation and emission spectra of the $Y_3(Al,Ga)_5O_{12}:Ce^{3+}$ phosphor powder.

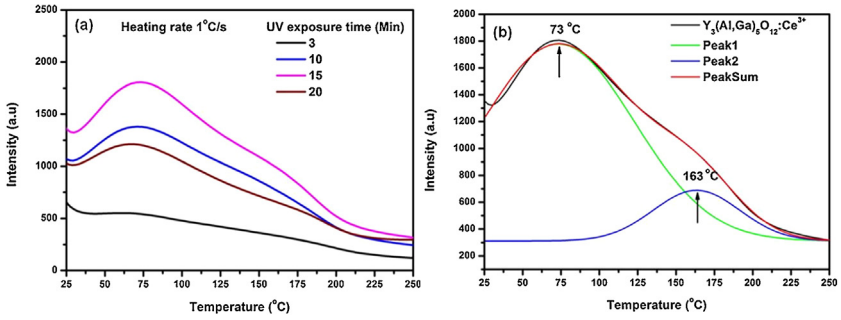

Fig. 3. (a) Glow curves showing TL variation with UV radiation time (b) Deconvolution of peaks 1 and 2.

ground state of activator ions are raised to the conduction band (CB) of $Y_3(Al,Ga)_5O_{12}:Ce^{3+}$ where they propagate. Some of the excited electrons relax and maybe captured by a trapping defect, Al/Ga substitutional defects or oxygen defects and are stored there. The holes resulting from this capture can also migrate in the VB and are trapped by Ce^{3+} ($Ce^{3+} + h^+ \rightarrow Ce^{4+}$). Upon thermal activation those electrons are released from the Al/Ga or oxygen defects back to the CB diffuse and relax to the excited state of the activators while the trapped hole is released back to the VB; this initiates a reverse process in which the hole recombines with the electron in the shallow Ce^{3+} (Ce^{4+}) site yielding the characteristic Ce^{3+} fluorescence emission [6,17]. If electron-hole pairs recombine immediately and emit a photon it is known as fluorescence [18] which explains the fluorescence nature of Ce^{3+}. Trapping from the conduction band to shallow traps or from shallow traps to deep traps can be the cause of the fast decay.

The peak at around 163 °C which might be equivalent to a deeper trap could therefore be attributed to traps arising from Al/Ga substitution defects induced by lattice disorder due to the difference between the ionic radii of Al^{3+} and Ga^{3+}. Ga^{3+} acts to provide hole-trap by occupying the Al^{3+} vacancy sites and this would mean distorted Ce^{3+} sites, which would act as a trap for excited Ce^{3+} electrons. The electron–hole recombination mediated by deep trap states within the band gap may be responsible for a slower decay component. It was reported elsewhere that the presence of shallow traps was detrimental to scintillation performance of $Lu_3Al_5O_{12}:Ce^{3+}$ [19] a problem which was overcome by tailoring the composition by introducing Ga^{3+} into the band gap of the $Lu_3Al_5O_{12}:Ce^{3+}$ a strategy that favored positioning of the $5d^1$ level of Ce^{3+} [20]. Since the density or amount of the traps and the rate of decay corresponds to the peak intensity of the glow curve, the electronic relaxation in $Y_3(Al,Ga)_5O_{12}:Ce^{3+}$ has a dominant fast luminescence decay due to a higher concentration of charge carrier captured in the shallow trap sites around 74 °C and a slower less dominant decay component due to deep trapping around 163 °C. Thus substitution of Ga^{3+} into the YAG:Ce^{3+} reduces the number of traps and lowers the TL signal. Previous studies have shown that substitution of Gd^{3+} for the rare-earth ion (Lu^{3+} or Y^{3+}) lowers the TL signal while samples with Y^{3+} have lower TL compared to those with Lu^{3+} [2]. Mutual change in the shape and intensity of the peaks corresponding to shallow traps in a glow curve compared with that of deeper traps may indicate the existence of inter-trap charge transfer. Electrons de-trapped from the shallower trap may be captured by the deeper trap or luminescence center as the temperature is raised [21].

3.4. UV exposure

From Fig. 4(a) we observe that with increasing UV irradiation/exposure time from 3 to 20 min, the position of the thermal peak maximum (T_m) of the glow curves shifted to higher temperatures and then to the lower temperatures. The shift in the TL peaks can be attributed to be due to the different rates at which the traps get filled [22]. This shift is also an indication that second order recombination kinetics could be taking place in which case a re-trapping process of the excitation occurs. First order kinetics occurs when the glow curve maximum (T_m) is independent of the dose absorbed by the material [6,23,24] such that the first order kinetic equations for the calculation of relevant trapping parameters may be applicable. A part from the variation of T_m, the shape of the glow curve can also give an indication of the order of kinetics whereby it is asymmetrical for first order and symmetrical for second order respectively. However the symmetrical shape or broadness of a glow curve may also be because of the presence of other several overlapping first order peaks and not due to the existence of second order kinetics [23].

A sharp rise in the TL maximum intensity (I_m) was observed for the dominant peak as shown in Fig. 4(b). The TL intensity initially increased with increase in irradiation time and tends to saturate at 10 min and then drops with further exposure.

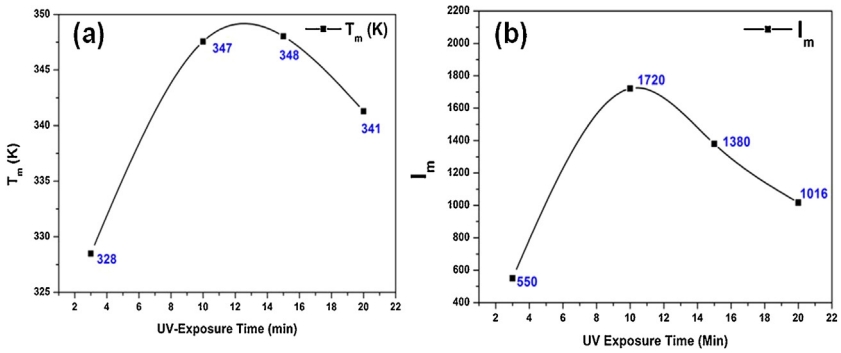

Fig. 4. Variation of (a) T_m (K) and (b) I_m with UV exposure time.

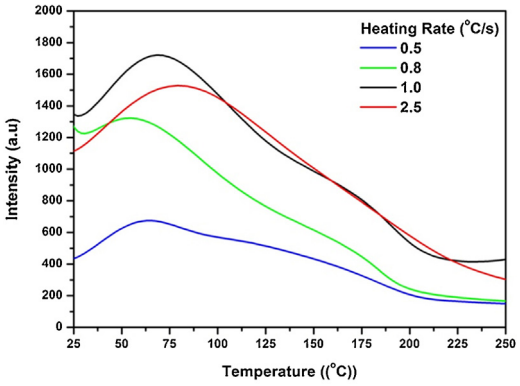

Fig. 5. TL glow curves showing the effect of heating rate variation as a function of temperature.

3.5. Heating rate method

The TL glow curves of $Y_3(Al,Ga)_5O_{12}:Ce^{3+}$ under different heating rates (β) are shown in Fig. 5.

The maximum temperature peak position (T_m) shifted to a higher temperature when the heating rate was increased as seen in Fig. 6(a). Similarly the Peak intensity (I_m) increased linearly with the heating rate as seen in Fig. 6(b).

Due to the shift of T_m to a higher temperature when the heating rate β (in °C/s) increased, we employed the Hoogenstraaten method which relates the TL peak temperature (T_m) and heating rate (β) [9,25,26] using the following equation:

$$\ln\left(\frac{T_m^2}{\beta}\right) = \frac{E}{kT_m} + \ln\left(\frac{E}{sk}\right) \quad (1)$$

to determine the activation energy, or trap depth where E is the activation energy or trap depth, k is the Boltzmann constant, β is the heating rate, s the frequency factor in s^{-1} and T_m represents the glow peak temperature. The resultant plot of $\ln(T_m^2/\beta)$ versus $1/kT_m$ also known as Hoogenstraaten plot, yields a straight line with slope E and intercept, $\ln(E/sK)$. Fig. 6(a) and (b) shows the Hoogenstraaten plots calculated from the TL glow curve of the $Y_3(Al,Ga)_5O_{12}:Ce^{3+}$ phosphor at different heating rates. Both the lower and higher temperature side peaks showed a linear relationship. The plots of the dominant lower temperature side peak gave a slope of 0.39 ± 0.08 eV as the trap depth as compared to 0.74 ± 0.15 eV calculated from slope of the less dominant peak on the higher temperature side (Fig. 7).

In this result, the depth of trap 1, attributed to be originating from Ce^{3+} ion incorporation, was 0.39 ± 0.08 eV and the depth of Trap 2, due to Ga^{3+} ion substitution, was 0.74 ± 0.15 eV. This clearly supports the idea that Ce^{3+} form shallow traps and hence decays faster as compared with the emission due to Ga^{3+} ion substitution which forms too deep trap from which emission may not be realized at all. The corresponding frequency factors s (s^{-1}) calculated from the intercept, $\ln(E/sK)$ of Eq. (1) were 2.93×10^4 s^{-1} and 1.2×10^8 s^{-1} for trap 1 and trap 2 respectively.

3.6. Peak shape method

Due to the symmetrical nature of the glow curves, and for comparison we also used Chen's second order kinetic equation [27],

$$E = 3.54\left(\frac{KT_m^2}{\omega}\right) - 2KT_m \quad (2)$$

based on the peak shape method to estimate the activation energy needed to de-trap charge carriers from the trap centers, where E is the activation energy/trap depth in eV, $k = 8.617 \times 10^{-5}$ eVK^{-1} is the Boltzmann's constant, T_m is the temperature corresponding to the maxima of a thermal peak and ω is the FWHM of the glow curve. The symmetry factor ($\mu = \delta/\omega = (T_2 - T_m)/(T_2 - T_1)$) (where T_m is the peak temperature at maximum intensity, T_1 and T_2 the lower- and upper-temperatures at half intensity) has been found to be approximately 0.52 for all glow curves, which indicates

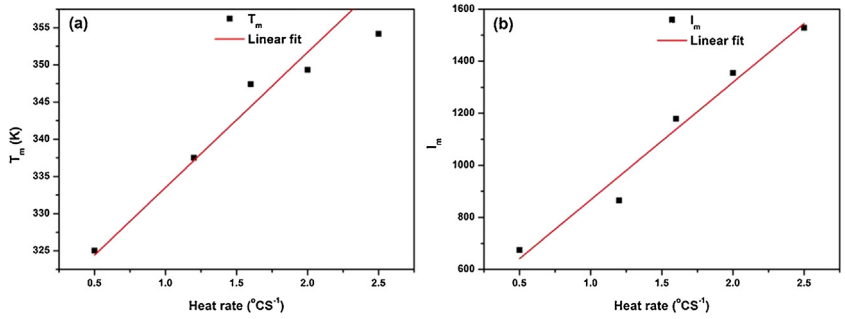

Fig. 6. Variation of (a) T_m and (b) I_m with heating rate.

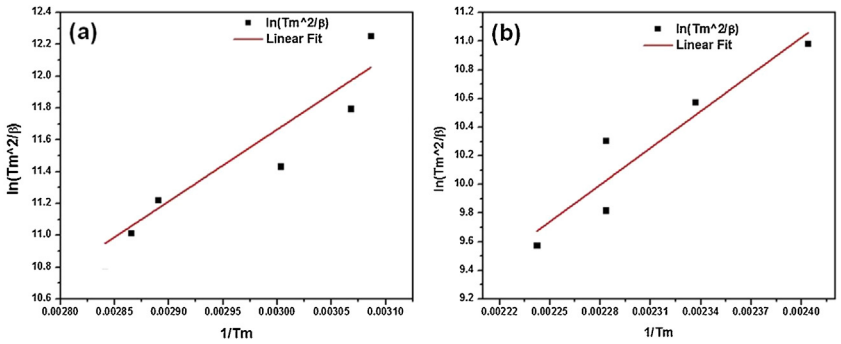

Fig. 7. Hoogenstraaten plots showing the dependence of the peak temperatures (T_m) of the $Y_3(Al,Ga)_5O_{12}:Ce^{3+}$ glow curves on the temperature-raising rate (β) for (a) trap 1 and (b) trap 2 respectively.

Table 1
Characteristic parameters of traps associated with TL peaks in $Y_3(Al,Ga)_5O_{12}:Ce^{3+}$.

	T_m (K)	E_t (eV)	Freq. factor (s)						
			0.5 °C/s	0.8 °C/s	1 °C/s	1.2 °C/s	1.6 °C/s	2 °C/s	2.5 °C/s
Peak 1									
	324	0.24	$6.42E^{06}$	$1.03E^{07}$	$1.28E^{07}$	$1.54E^{07}$	$2.05E^{07}$	$2.57E^{07}$	$3.21E^{07}$
	326	0.20	$1.36E^{05}$	$2.17E^{05}$	$2.72E^{05}$	$3.26E^{05}$	$4.35E^{05}$	$5.44E^{05}$	$6.80E^{05}$
	342	0.25	$3.86E^{06}$	$6.18E^{06}$	$7.72E^{06}$	$9.27E^{06}$	$1.24E^{07}$	$1.54E^{07}$	$1.93E^{07}$
	333	0.21	$2.41E^{05}$	$3.86E^{05}$	$4.83E^{05}$	$5.79E^{05}$	$7.73E^{05}$	$9.66E^{05}$	$1.21E^{06}$
	346	0.23	$5.50E^{05}$	$8.80E^{05}$	$1.10E^{06}$	$1.32E^{06}$	$1.76E^{06}$	$2.20E^{06}$	$2.75E^{06}$
	349	0.21	$1.04E^{05}$	$1.66E^{05}$	$2.07E^{05}$	$2.49E^{05}$	$3.31E^{05}$	$4.14E^{05}$	$5.18E^{05}$
	352	0.22	$2.04E^{05}$	$3.23E^{05}$	$4.07E^{05}$	$4.89E^{05}$	$6.52E^{05}$	$8.14E^{05}$	$1.02E^{06}$
Average		0.23	$1.64E^{06}$	$2.63E^{06}$	$3.29E^{06}$	$3.95E^{06}$	$5.26E^{06}$	$6.58E^{06}$	$8.22E^{06}$
Peak 2									
	416	0.69673	$5.69E^{17}$	$9.11E^{17}$	$1.14E^{18}$	$1.37E^{18}$	$1.82E^{18}$	$2.28E^{18}$	$2.85E^{18}$
	428	0.77264	$1.96E^{19}$	$3.13E^{19}$	$3.91E^{19}$	$4.69E^{19}$	$6.26E^{19}$	$7.82E^{19}$	$9.78E^{19}$
	438	0.86445	$1.89E^{21}$	$3.03E^{21}$	$3.78E^{21}$	$4.54E^{21}$	$6.05E^{21}$	$7.57E^{21}$	$9.46E^{21}$
	424	0.59787	$3.92E^{14}$	$6.27E^{14}$	$7.84E^{14}$	$9.41E^{14}$	$1.25E^{15}$	$1.57E^{15}$	$1.96E^{15}$
	438	0.91235	$3.72E^{22}$	$5.96E^{22}$	$7.45E^{22}$	$8.93E^{22}$	$1.19E^{23}$	$1.49E^{23}$	$1.86E^{23}$
	446	0.90656	$9.28E^{21}$	$1.48E^{22}$	$1.86E^{22}$	$2.23E^{22}$	$2.97E^{22}$	$3.71E^{22}$	$4.64E^{22}$
	448	0.76985	$1.74E^{18}$	$2.79E^{18}$	$3.48E^{18}$	$4.18E^{18}$	$5.57E^{18}$	$6.97E^{18}$	$8.71E^{18}$
Average		0.79	$6.92E^{21}$	$1.11E^{22}$	$1.38E^{22}$	$1.66E^{22}$	$2.21E^{22}$	$2.77E^{22}$	$3.46E^{22}$

second order kinetics [28]. From the equation and the shape of the glow curve it can be inferred that the rate of thermal activation is proportional to the rate of thermal release of the trapped charge carriers [14]. The corresponding frequency factor s (s^{-1}) which is the frequency of an electron escaping the trap can be calculated using the Garlick and Gibson second order kinetics formula [29] as given in Eq. (3);

$$S = \frac{\beta E}{kT_m^2}\frac{1}{1+\frac{2kT_m}{E}}\exp\left(\frac{E}{kT_m}\right) \quad (3)$$

The values of the activation energies and frequency factors for trap 1 and 2 calculated from some of the glow curves at different heating rates using Eqs. (2) and (3) are presented in Table 1.

The calculated values of trap depth (E_t) which is similar to the activation energy, gave an average of 0.23 ± 0.1 eV and 0.79 ± 0.1 eV for trap 1 and 2 respectively. The value for peak 2 is quite comparable with 0.74 eV calculated from the Hoogenstraaten method using Eq. (1).

3.7. TL Anal GCD method

To further estimate the actual trap depths, a deconvolution of the glow curves with second order kinetics was carried out using a TL Anal GCD program. Fig. 8 shows the deconvoluted glow curves for the different heating rates.

The values of the activation energies and frequency factors for trap 1 and 2 estimated using TL Anal software for the different heating rates are given in Table 2.

This method gave values of trap depth (E_t) as 1.59 ± 0.1 eV and 2.14 ± 0.1 eV for trap 1 and 2 respectively. The corresponding frequency factors s (s^{-1}) were 7.61×10^{18} s^{-1} and 6.9×10^{20} s^{-1} for trap 1 and trap 2 almost in the same range as reported by Pitale et al. using CGCD procedure [23]. The trap depths obtained in our results using the TL Anal GCD method are larger than those we obtained by Hoogenstraaten and peak shape methods. The discrepancy may be attributed to be as a result of a continuous trap depth distribution which deforms the glow peaks and makes the simple glow peak models ill-suited. However it is still that assumed the figures due to Hoogenstraaten's method to be most reliable [30]. In another study, Piters et al. also reported that although in some cases the deviation between the heating rate method and glow curve fitting method can be quite significant, the Hoogenstraaten's heating rate method remains a generally reliable method for determining TL trapping parameters of first order glow peaks. In their study they attributed the deviation to be due to a systematic increase of a temperature lag between the measured and real temperature of the sample (i.e. non-ideal heat transfer between heating element and sample) as the heating rate increased which affects the linear part of the heating rates plots more than has been previously realized. They concluded that the effect of the temperature lag on Hoogenstraaten's heating rate method is a decrease in activation energy and frequency factor and is more important

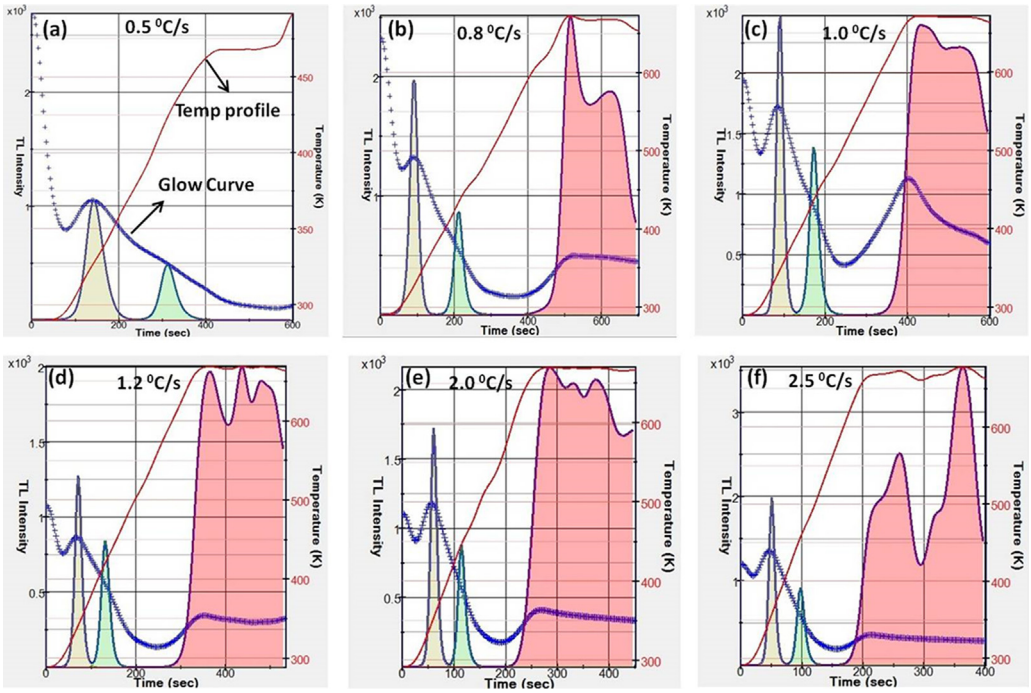

Fig. 8. Deconvolution of the TL glow curve of the $Y_3(Al,Ga)_5O_{12}:Ce^{3+}$ powder with second order kinetics using TL Anal GCD program.

Table 2
Characteristic parameters of traps associated with TL peaks in $Y_3(Al,Ga)_5O_{12}:Ce^{3+}$.

Heating rates (°C/s)	Trap depth1 E_t (eV)	Freq. factor s (s^{-1})	Trap depth2 E_t (eV)	Freq. factor s (s^{-1})
0.5	1.43	1.20E^{16}	2.03	4.59E^{18}
0.8	1.59	7.0E^{18}	2.09	6.68E^{18}
1.0	1.73	3.48E^{19}	1.92	3.71E^{16}
1.2	1.58	1.56E^{18}	2.04	2.05E^{19}
1.6	1.51	2.37E^{16}	2.31	1.39E^{21}
2.0	1.57	1.35E^{17}	2.13	3.80E^{18}
2.5	1.72	9.75E^{18}	2.49	3.43E^{21}
Average	1.59	7.61E^{18}	2.14	6.94E^{20}

for glow peaks with high activation energy and high frequency factor [31].

Also Sunta et al. reported that the peak shape, general order peak fitting and initial rise methods of determining E values of TL glow peaks produce low values. In the peak shape and general order fitting methods this happens when the retrapping probability is much higher than the recombination probability and the sample dose is higher thereby filling the traps up to near the saturation level. In the case of initial rise method it was because the exponential growth region of the TL intensity may be too weak to be measured above the instrumental background. The proposed the use of low sample doses for analysis of the glow peaks as a remedy for these discrepancies [32].

4. Conclusion

In this study we performed TL measurements on commercial $Y_3(Al,Ga)_5O_{12}:Ce^{3+}$ phosphor. Each of the glow curves consisted of two thermal peaks indicating existence of more than one type of trap; one of them is centered at 74 °C and the other on the higher temperature side at 163 °C corresponding to shallow and deep traps respectively. With increasing UV exposure time the position of the thermal peak maximum (T_m) of the glow curves shifted to higher temperatures and then to the lower temperatures. The TL intensity initially increased with an increase in UV exposure time and tends to saturate at after 10 min and then dropped with further exposure. The maximum temperature peak position (T_m) shifted to higher temperature when the heating rate was increased. The depth of trap 1, originating from Ce^{3+} ion was 0.39 ± 0.08 eV and the depth of Trap 2, originating from Ga^{3+} ion substitution, was 0.74 ± 0.15 eV as calculated from the Hoogenstraaten method. Values of trap depth (E_t) calculated using Chen's peak shape method gave an average of 0.23 ± 0.1 eV and 0.79 ± 0.1 eV for trap 1 and 2 respectively which was quite comparable to 0.74 eV for trap 2 calculated from the Hoogenstraaten method. We observed that trap depths obtained with the TL Anal GCD method were much larger than those obtained by Hoogenstraaten and peak shape methods. The difference may be attributed to be a result of a continuous trap depth distribution which deforms the glow peaks and makes the simple glow peak models ill-suited. However it is still assumed that the figures due to Hoogenstraaten's method to be the most reliable.

Acknowledgement

The authors acknowledge with immense gratitude the South African Research Chairs Initiative of the Department of Science and Technology, the National Research Foundation of South Africa and University of the Free State Cluster Fund.

References

[1] J. Li, J.-G. Li, Z. Zhang, X. Wu, S. Liu, X. Li, X. Sun, Y. Sakka, Sci. Technol. Adv. Mater. 13 (2012) 035007.
[2] E. Mihóková, K. Vávr, K. Kamada, V. Babin, A. Yoshikawa, M. Nikl, Radiat. Meas. 56 (2013) 1.
[3] I. Bailiff, J. Archaeol. Sci. 18 (1991) 619.
[4] M. Ziyauddin, N. Brahme, D.P. Bisen, R.S. Kher, Recent Res. Sci. Technol. 4 (2012) 95.
[5] N.L. Hom, Preparation and Properties of Long Persistent $Sr_4Al_{14}O_{25}$ Phosphors Activated by Rare Earth Metal Ions, Saga University, 2010.
[6] F. You, A.J.J. Bos, Q. Shi, S. Huang, J. Phys.: Condens. Matter 23 (2011) 215502.
[7] D.S. Kshatri, A. Khare, P. Jha, Chalcogenide Lett. 10 (2013) 121.
[8] H. Yamamoto, T. Matsuzawa, J. Lumin. 2313 (1997) 72.
[9] P. Dorenbos, J. Electrochem. Soc. 152 (2005) H107.
[10] R. Chen, Y. Wang, Y. Hu, Z. Hu, C. Liu, J. Lumin. 128 (2008) 1180.

[11] V. Dubeya, S. Agrwal, J. Kaur, Optik 126 (2015) 1.
[12] A.H. Wako, B.F. Dejene, H.C. Swart, Phys. B: Condens. Matter 439 (2014) 153.
[13] G. Kitis, J.M. Gomez-Ros, J.W.N. Tuyn, J. Phys. D.: Appl. Phys. 31 (1999) 2636.
[14] L.L. Noto, S.S. Pitale, M.A. Gusowki, J.J. Terblans, O.M. Ntwaeaborwa, H.C. Swart, Powder Technol. 237 (2013) 141.
[15] A. Bril, G. Blasse, J. de Poorter, J. Electrochem. Soc. 117 (1970) 346.
[16] P.A. Tanner, L. Fu, L. Ning, B.-M. Cheng, M.G. Brik, J. Phys.: Condens. Matter 19 (2007) 216213.
[17] A. Potdevin, G. Chadeyron, V. Briois, R. Mahiou, Mater. Chem. Phys. 130 (2011) 500.
[18] C. Burda, X. Chen, R. Narayanan, M.A. El-sayed, Chem. Rev. 105 (2005) 1025.
[19] M. Nikl, E. Mihokova, J.A. Mares, A. Vedda, K. Nejezchleb, K. Blazek, Phys. Status Solidi 181 (2000) 10.
[20] M. Fasoli, A. Vedda, M. Nikl, C. Jiang, B.P. Uberuaga, D.A. Andersson, K.J. McClellan, C.R. Stanek, Phys. Rev. B.: Condens. Matter Mater. Phys. 84 (2011).
[21] S. Basun, G.F. Imbusch, D.D. Jia, W.M. Yen, J. Lumin. 104 (2003) 283.
[22] T. Aitasalo, J. Holsa, M. Lastusaari, J. Niittykoski, J. Phys. Chem. B 110 (2006) 4589.
[23] S.S. Pitale, S.K. Sharma, R.N. Dubey, M.S. Qureshi, M.M. Malik, Nucl. Instrum. Methods Phys. Res. B 266 (2008) 2027.
[24] A. Choubey, S.K. Sharma, S.P. Lochab, D. Kanjilal, Radiat. Eff. Defects Solids 166 (2011) 487.
[25] P. Avouris, J. Chem. Phys. 74 (1981) 4347.
[26] Y. Kojima, K. Aoyagi, T. Yasue, J. Lumin. 126 (2007) 319.
[27] R. Chen, J. Appl. Phys. 40 (1969) 570.
[28] G. Kitis, V. Pagonis, Nucl. Instrum. Methods Phys. Res. B 262 (2007) 313.
[29] P.K. Suan, Thermoluminescence Studies of Naturally Occurring Salts Relevant to Dosimtery Obtained from Mizoram, Mizoram University, 2013.
[30] L. Puust, V. Kiisk, K. Utt, H. Mändar, I. Sildos, Cent. Eur. J. Phys. 12 (2014) 415.
[31] T.M. Piters, R. Melendrez, W. Drozdowski, Radiat. Prot. Dosim. 84 (1999) 127.
[32] C.M. Sunta, A.W.E. Feria, T.M. Piters, S. Watanabe, Radiat. Meas. 30 (1999) 197.